Acta Crystallographica Section B
Structural Science
ISSN 0108-7681

Structure and complex twinning of dysprosium disilicate ($Dy_2Si_2O_7$), Type B

Michael E. Fleet* and Xiaoyang Liu

Department of Earth Sciences, University of Western Ontario, London, Ontario, Canada N6A 5B7

Correspondence e-mail: mfleet@julian.uwo.ca

Received 23 February 2000
Accepted 16 June 2000

Dysprosium disilicate ($Dy_2Si_2O_7$) is triclinic with a = 6.6158 (2), b = 6.6604 (2), c = 12.0551 (4) Å, α = 94.373 (2), β = 90.836 (2), γ = 91.512 (2)°, V = 529.4 (1) Å^3, space group $P\bar{1}$, Z = 4 and D_x = 6.156 g cm^{-3}. The structure (single-crystal X-ray, R = 0.033, wR = 0.041) is built from a linear triple tetrahedral group [Si_3O_{10}] and isolated [SiO_4] tetrahedron cross-linked by Dy^{3+} in one sixfold and three eightfold coordinated positions, and corresponds to the presently revised type B structure of $Ho_2Si_2O_7$. The formation of the unusual linear triple tetrahedral group in the type B structure allows for a more continuous transition in the mean size of $REE^{3+}O_n$ (REE = rare earth element) polyhedra in REE disilicates through the 4*f* transition metal series. The crystal of $Dy_2Si_2O_7$ investigated was complexly twinned such that the diffraction pattern was also consistent with a larger dimensionally monoclinic unit cell (a = 22.5354, b = 14.2102, c = 6.6158 Å, β = 91.788°), which resulted in an apparent superstructure of the type B structure in space group $C\bar{1}$. Lattice coincidence with the type B unit cell appears to have been maintained during crystal synthesis and quenching by the complex sector-zoned growth twin.

1. Introduction

The structures of the single rare earth element (REE) disilicates vary with both position in the lanthanide series (or size of the REE^{3+} cation) and temperature, at room pressure. Seven distinct structure types (A–G) have been identified (Felsche, 1970*a*) and reported on (Felsche, 1970*b*,*c*; Smolin & Shepelev, 1970; Smolin *et al.*, 1970; Felsche, 1971, 1972; Greis *et al.*, 1991; Dias *et al.*, 1990; Christensen, 1994; Christensen & Hazell, 1994; Christensen, Hazell & Hewat, 1997; Christensen, Jensen *et al.*, 1997). The triclinic type B structure is adopted by dysprosium disilicate ($Dy_2Si_2O_7$), below ~1748 K, as well as by the disilicates of neighbouring REE (Eu, Gd, Tb, Ho and Er). At higher temperature, $Dy_2Si_2O_7$ crystallizes with the orthorhombic type E structure, as do the disilicates of Eu, Gd, Tb and Ho. Unlike the other six known structure types, in which the [SiO_4] tetrahedra are associated into diorthosilicate [Si_2O_7] groups, the type B structure reported by Felsche (1972) for $Ho_2Si_2O_7$ was very unusual in having the [SiO_4] tetrahedra in a one-to-one combination of a single (isolated) tetrahedron and a linear triple tetrahedral group [Si_3O_{10}]. A second unusual feature of this structure was the high degree of distortion of the [SiO_4] tetrahedra, for which individual Si—O bond lengths varied from 1.56 to 1.78 Å.

2. Procedures

Single crystals of $Dy_2Si_2O_7$ were encountered as a by-product in an experiment to synthesize crystals of Dy-bearing chlorapatite [$Ca_{9.74}Na_{0.14}Dy_{0.14}(PO_4)_6Cl_2$; Fleet *et al.*, 2000]. A Ca–Dy silicate starting composition of stoichiometry $Ca_4Dy_6(SiO_4)_6Cl_2$ was prepared from $CaCO_3$, Dy_2O_3, SiO_2 and $CaCl_2$. The charge consisted of ~0.030 g of the starting composition, 0.01 g of NaCl, 0.030 g of a mixture of $CaCl_2{\cdot}H_2O$ and P_2O_5 in the stoichiometric proportion of $Ca_{10}(PO_4)_6Cl_2$, and 0.01 g of deionized water contained in a sealed gold capsule 3.5 cm in length. It was heated initially to ~1183 K at 0.2 GPa, then cooled to 1008 K at 0.3 K min^{-1}, maintained at 1008 K and 0.10 GPa for 13 h, and quenched in air and water. The products were digested in hot water, and washed several times in cold water.

Dysprosium disilicate was characterized by powder and single-crystal X-ray diffraction and electron probe microanalysis (EPMA). The latter was made with a Jeol 8600 Superprobe and gave Dy_2O_3 = 75.2 (4), SiO_2 = 23.8 (4), CaO = 0.43 (9), Na_2O = 0.21 (2), P_2O_5 = 0.08 (7), Cl_2 = 0.03 (1), total = 99.7 wt% (average of 18 microprobe spot analyses). Operating conditions included an accelerating voltage of 20 kV, a beam current of 15 nA, a beam diameter of 2 μm, 20 s counts, and $DyPO_4$, albite ($NaAlSi_3O_8$), Durango apatite, and sodalite ($Na_4Al_3Si_3O_{12}Cl$) as standards, and the measurements were reduced using the Love–Scott model (Sewell *et al.*, 1985).

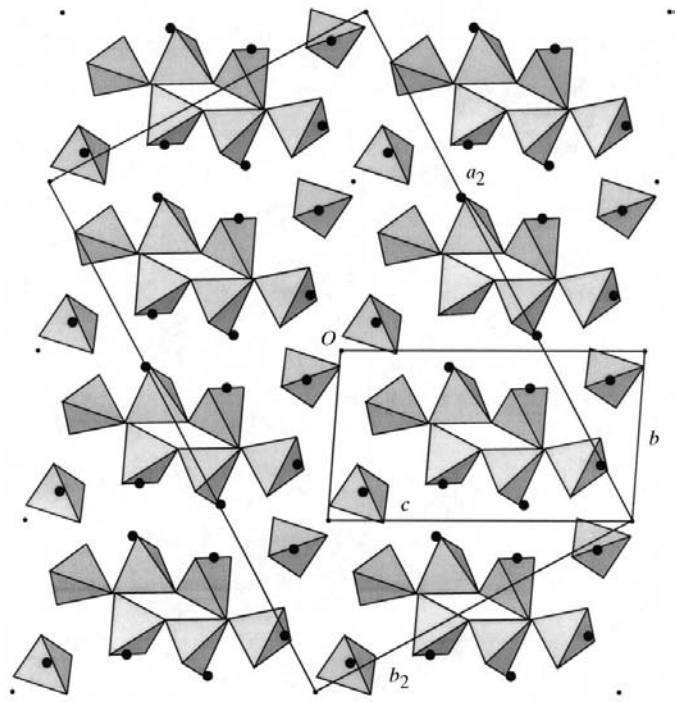

Figure 1
Geometric relationship of unit cells of the triclinic type B structure of $Dy_2Si_2O_7$ (b, c) and dimensionally monoclinic $C\bar{1}$ pseudostructure (a_2, b_2); see text for transformation matrices; O is the unit-cell origin for the type B structure reported in Table 1; $[100]_{\text{type B}}$ projection; note that b, c and a_2 edge lengths are distorted by the projection; drawn with *ATOMS* (Dowty, 1995).

Dysprosium appeared to be present in excess of the stoichiometric proportion (Dy:Si = 1.019), but this was probably related to difficulty in calibrating a large amount of this heavy element. Also, the substitution mechanism for incorporation of minor amounts of Ca and Na was not obvious.

The crystals of $Dy_2Si_2O_7$ were colourless, approximately rhombic prismatic and sector twinned, and had monoclinic crystal optics and diffraction symmetry [a = 22.5354 (7), b = 14.2102 (5), c = 6.6158 (2) Å, β = 91.788 (2)°]. This monoclinic unit cell was used for collection of reflection intensities and data reduction. *SHELXTL/PC* (Siemens, 1993) resulted in a twinned structure solution, from which a unique triclinic structure in space group $C\bar{1}$, but with the dimensionally monoclinic unit cell, was extracted by iteration. The $C\bar{1}$ structure was recognized as a simple multiple (4 ×) of the type B structure of $Ho_2Si_2O_7$ (Felsche, 1972); matrices for transformation from $C\bar{1}$ to type B (P) being /0, 0, 1; 0.25, −0.25, 0; 0.25, 0.75, 0/ for reflections and /0, 0, 1; 3, −1, 0; 1, 1, 0/ for atomic coordinates (Fig. 1). Unit-cell parameters for the type B structure were extracted from the transformation matrix /43.7688, −1.1630, −1.1630; −1.1630, 44.3609, −6.1216; −1.1630, −6.1216, 145.3259/.

3. Discussion

3.1. Twinning

All single crystals of $Dy_2Si_2O_7$ were sector twinned (Fig. 2) with composition planes (010) and (100), referring to the large ($C\bar{1}$) unit cell (Table 1), which we have noted is dimensionally monoclinic. Twin individuals were related by reflection on (010) and 180° rotation around the b axis, which are the twin operations of the familiar albite and pericline twin laws, respectively, of feldspar minerals. The rhombic section of the pericline twin was parallel to the c axis, consistent with $\alpha = \gamma = 90°$ (Tunell, 1952). All four twin sectors were uniformly extinguished with (010) parallel to the direction of polarization of the petrographic microscope, consistent with monoclinic crystal optics. However, the extinction lingered in opposed sectors when the microscope stage was rotated on either side of the position of extinction, as depicted in Fig. 2, which suggested that the central region of crystals was strained. The $C\bar{1}$ structure was refined by correcting the observed structure factors of reflection pairs hkl and $h\bar{k}l$ for the contribution from twinning after the procedure of Fleet & Burns (1990), using equal proportions of the two twin orientations. Reflections $h0l$ were unaffected by the twinning, confirming the identification of (010) as the twin plane.

The (010) twin plane of the triclinic $C\bar{1}$ structure corresponds to ($0\bar{1}3$) of the type B ($P\bar{1}$) structure (Fig. 1). Also, hkk in the reciprocal lattice of type B corresponds to h_20l_2, with $h_2 = 4k$ and $l_2 = h$, in the reciprocal lattice of $C\bar{1}$, which is now labelled with subscripted indices. The 4470 reflections used in refinement of the type B structure belonged to three classes of reflections distinguished in the manner in which they were affected by the twinning. Relative to the triclinic unit cell of the type B structure, the first class comprised 144 hkk reflec-

Table 1
Unit-cell parameters for $Dy_2Si_2O_7$ and $Ho_2Si_2O_7$.

1: calculated from (2); 2: measured on a twinned crystal (this study); 3: powder X-ray diffraction (Felsche, 1970*a*); 4: calculated from (3); 5: real space unit-cell edge lengths and reciprocal space angles (Felsche, 1972); 6: revised real space parameters; 7: calculated from (6).

	$Dy_2Si_2O_7$				$Ho_2Si_2O_7$		
	1 Type B	2 $C\bar{1}$	3 Type B	4 $C\bar{1}$	5 Type B	6 Type B	7 $C\bar{1}$
a (Å)	6.616	22.535	6.639	22.722	6.612	6.612	22.605
b (Å)	6.66	14.21	6.691	14.278	6.669	6.669	14.223
c (Å)	12.055	6.616	12.152	6.639	12.085	12.085	6.612
α (°)	94.37	90	94.03	89.63	85.81	94.19	90.11
β (°)	90.84	91.79	89.81	91.38	89.38	90.62	91.6
γ (°)	91.51	90	91.69	89.66	88.57	91.43	89.85

tions that were unaffected by the twinning. The second class comprised 2228 reflections derived from twin reflection pairs hk_al_a and hk_bl_b with $(k_a - l_a) = (l_b - k_b) = 2n + 1$, and either k_a and l_a or k_b and l_b fractional; *i.e.* only one of each twin pair of $C\bar{1}$ reciprocal lattice points transformed to a lattice point of type B. Correction for twinning was made by doubling $F_{hkl}{}^2$ of the type B reflection. The third class comprised 2098 reflections derived from twin reflection pairs hk_al_a and hk_bl_b with $(k_a - l_a) = (l_b - k_b) = 2n$. Both of each twin pair of lattice points transformed from $C\bar{1}$ corresponded to lattice points of the type B structure and, therefore, type B reflection intensities were complexly overlapped. Correction was made, as above, following the procedure of Fleet & Burns (1990). Finally, there were 2243 other $C\bar{1}$ reciprocal lattice points that did not transform to lattice points of the type B structure and, thus, afforded a potentially unambiguous indication of whether the $C\bar{1}$ structure was a true superstructure of the type B structure or merely a product of lattice coincidence. The latter was strongly indicated because only four of these 2243 reflections had $I \leq 3\sigma(I)$.

From its morphology and well defined composition planes (Fig. 2), the $Dy_2Si_2O_7$ twin appears to have developed during crystal growth, and likely maintained the dimensional correspondence between the pseudomonoclinic $C\bar{1}$ and type B crystal lattices over the temperature range of the crystal growth and during subsequent quenching. The minor differential strain in twin sectors evident in the crystal optics probably reflects some relaxation of twin coherence, but this was not evident in the diffraction data. Interestingly, the unit cell of the $Ho_2Si_2O_7$ crystal investigated by Felsche (1972) shows close to dimensional correspondence with the pseudomonoclinic $C\bar{1}$ structure (Table 1). The unit-cell parameters of the type B structures of the disilicates of Eu, Gd, Tb, Dy, Ho and Er given in Felsche (1970*a*) are further removed from dimensional correspondence with the $C\bar{1}$ structure. However, these data were determined by powder XRD and are more likely to be affected by systematic errors.

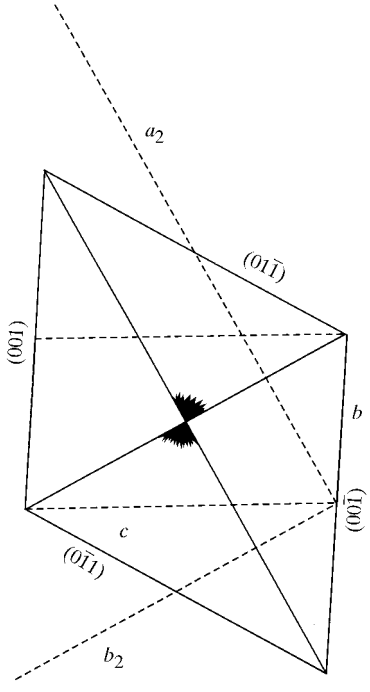

Figure 2
Sketch of the sector-twinned crystal of $Dy_2Si_2O_7$, relative to unit cells of the type B structure (b, c) and $C\bar{1}$ pseudostructure (a_2, b_2): shading indicates the strain extinction of sectors in crystallographic continuity.

3.2. Type B structure

The crystal used for the present study was strained by partial relaxation of the twin coherence (Fig. 2) and this undoubtedly contributed to the rather high value of R_{int} (0.11; Table 2).[1] Error in the absorption correction, which followed

[1] Supplementary data for this paper are available from the IUCr electronic archives (Reference: BR0099). Services for accessing these data are described at the back of the journal.

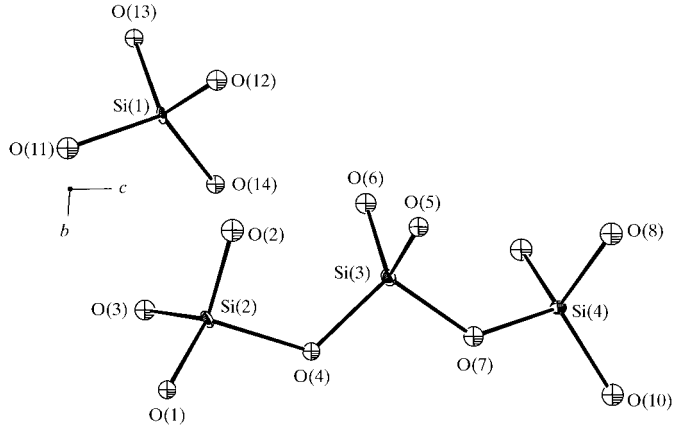

Figure 3
Linear triple tetrahedral group $[Si_3O_{10}]$ and isolated $[SiO_4]$ tetrahedron in type B structure of $Dy_2Si_2O_7$. Thermal ellipsoids for Si atoms are scaled to enclose 50% probability; a^*-axis projection; drawn with *ORTEP*3 (Farrugia, 1999).

Table 2
Experimental details.

Crystal data	
Chemical formula	$Dy_2Si_2O_7$
Chemical formula weight	493.17
Cell setting	Triclinic
Space group	$P\overline{1}$
a (Å)	6.6158 (2)
b (Å)	6.6604 (2)
c (Å)	12.0551 (4)
α (°)	94.373 (2)
β (°)	90.836 (2)
γ (°)	91.512 (2)
V (Å^3)	529.39
Z	4
D_x (Mg m^{-3})	6.156
Radiation type	Mo $K\alpha$
Wavelength (Å)	0.70926
No. of reflections for cell parameters	32 768
θ range (°)	2–35
μ (mm^{-1})	28.45
Temperature (K)	293 (2)
Crystal form	Prism
Crystal size (mm)	0.11 × 0.10 × 0.05
Crystal color	Colorless
Data collection	
Diffractometer	Nonius KappaCCD
Data collection method	Area detector and scans
Absorption correction	*Gaussian* (Coppens *et al.*, 1965)
T_{min}	0.144
T_{max}	0.380
No. of measured reflections	32 768
No. of independent reflections	4470
No. of observed reflections	3220
Criterion for observed reflections	$I \geq 3\sigma(I)$
R_{int}	0.107
θ_{max} (°)	35
Range of h, k, l	$-10 \rightarrow h \rightarrow 10$ $-5 \rightarrow k \rightarrow 9$ $0 \rightarrow l \rightarrow 19$
Refinement	
Refinement on	F
R	0.0325
wR	0.0407
S	0.978
No. of reflections used in refinement	4470
No. of parameters used	204
Weighting scheme	$w = 1/[\sigma(F)^2 + (0.025F)^2]$
$(\Delta/\sigma)_{max}$	0.0006345
$\Delta\rho_{max}$ (e Å^{-3})	4.65
$\Delta\rho_{min}$ (e Å^{-3})	−4.70
Extinction method	B–C type 1 Lorentzian isotropic
Extinction coefficient	0.31 (2)
Source of atomic scattering factors	*International Tables for X-ray Crystallography* (1974, Vol. IV, Tables 2.2A and 2.3.1)
Computer programs	
Data collection	*COLLECT* (Nonius, 1997)
Cell refinement	*COLLECT* (Nonius, 1997)
Data reduction	*DATAP*77 (Coppens, 1977*a*)
Structure solution	*SHELXTL*/*PC* (Siemens, 1993)
Structure refinement	*LINEX*77 (Coppens, 1977*b*)

Coppens *et al.* (1965), did not appear to make a significant contribution to R_{int}. The value of R_{int} before absorption correction was 0.22. Absorption correction using *SORTAV* (Blessing, 1995, 1997), which is integrated with *COLLECT* (Nonius, 1997), reduced R_{int} to only 0.13 and yielded an unsatisfactory refinement of the structure (R = 0.044, wR = 0.065, S = 1.98). Furthermore, the range in transmission factors reported in Table 2 is in good agreement with transmission factors estimated for spherical crystals of diameter 0.11 and 0.05 mm (0.15 and 0.36, respectively). The structure refinement was made with anisotropic displacement parameters for all atoms. However, the displacement parameters for O(4) (Fig. 3) were non-positive definite when rounded to significant figures, and the ellipsoids for O(3) and O(11) were excessively deformed as well. Evidently the anisotropic displacement parameters for O atoms were not physically realistic, their determination being limited by the high proportion of heavy atoms in the structure and the complexly twinned crystal.

Table 3
Fractional atomic coordinates and equivalent isotropic displacement parameters (Å^2).

$$U_{eq} = (1/3)\Sigma_i\Sigma_j U^{ij} a^i a^j \mathbf{a}_i.\mathbf{a}_j.$$

	x	y	z	U_{eq}
Dy(1)	0.94853 (4)	0.33132 (4)	0.11643 (2)	0.00588 (9)
Dy(2)	0.88556 (4)	0.09387 (4)	0.35971 (2)	0.00579 (9)
Dy(3)	0.37254 (4)	0.78116 (4)	0.36895 (2)	0.00749 (9)
Dy(4)	0.66787 (4)	0.82973 (4)	0.10747 (2)	0.00742 (9)
Si(1)	0.1553 (2)	0.8528 (2)	0.1164 (1)	0.0048 (3)
Si(2)	0.4873 (3)	0.3370 (2)	0.1759 (1)	0.0061 (3)
Si(3)	0.3777 (3)	0.2743 (2)	0.4048 (1)	0.0064 (3)
Si(4)	0.1433 (3)	0.3702 (2)	0.6180 (1)	0.0056 (3)
O(1)	0.6418 (6)	0.4938 (6)	0.1256 (3)	0.0076 (7)
O(2)	0.6179 (7)	0.1419 (6)	0.2095 (4)	0.0120 (8)
O(3)	0.2978 (7)	0.2990 (7)	0.0947 (3)	0.0097 (8)
O(4)	0.4055 (6)	0.4283 (6)	0.3065 (3)	0.0072 (7)
O(5)	0.5836 (7)	0.1702 (6)	0.4454 (4)	0.0090 (8)
O(6)	0.2276 (6)	0.0965 (6)	0.3755 (4)	0.0100 (8)
O(7)	0.2885 (7)	0.4229 (6)	0.5118 (3)	0.0093 (8)
O(8)	0.2841 (7)	0.2167 (7)	0.6875 (4)	0.0118 (8)
O(9)	0.9629 (7)	0.2255 (6)	0.5700 (4)	0.0113 (8)
O(10)	0.0732 (7)	0.5777 (6)	0.6854 (4)	0.0109 (8)
O(11)	0.2411 (7)	0.9129 (7)	0.9994 (3)	0.0111 (8)
O(12)	0.3462 (6)	0.7886 (7)	0.1888 (4)	0.0095 (8)
O(13)	0.9982 (6)	0.6683 (6)	0.0809 (3)	0.0077 (8)
O(14)	0.0029 (6)	0.0165 (6)	0.1830 (3)	0.0075 (7)

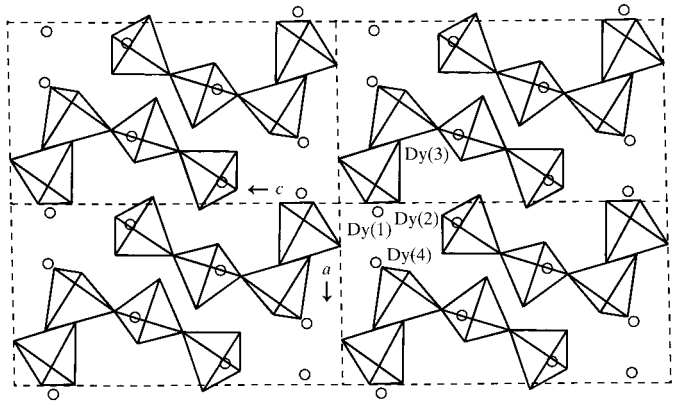

Figure 4
Polyhedral representation of the structure of type B of $Dy_2Si_2O_7$ locating Dy positions (open circles); [010] projection; drawn with *ORTEP*3 (Farrugia, 1999).

Table 4
Selected geometric parameters (Å, °).

Dy(1)—O(1)	2.325 (2)	Dy(2)—O(14^{i})	2.304 (4)
Dy(1)—O(2)	2.789 (3)	Dy(3)—O(4)	2.429 (4)
Dy(1)—O(3^{i})	2.343 (1)	Dy(3)—O(5^{ii})	2.250 (4)
Dy(1)—O(10^{ii})	2.427 (4)	Dy(3)—O(6^{vi})	2.328 (4)
Dy(1)—O(11^{ii})	2.380 (3)	Dy(3)—O(8^{ii})	2.381 (1)
Dy(1)—O(13)	2.333 (4)	Dy(3)—O(9^{ii})	2.348 (1)
Dy(1)—O(13^{iii})	2.410 (4)	Dy(3)—O(12)	2.181 (4)
Dy(1)—O(14^{i})	2.336 (4)	Dy(4)—O(1)	2.267 (4)
Dy(2)—O(2)	2.558 (3)	Dy(4)—O(2^{vi})	2.367 (4)
Dy(2)—O(5)	2.313 (2)	Dy(4)—O(3^{vii})	2.537 (4)
Dy(2)—O(6^{i})	2.267 (4)	Dy(4)—O(8^{ii})	2.531 (5)
Dy(2)—O(8^{iv})	2.354 (4)	Dy(4)—O(11^{viii})	2.295 (4)
Dy(2)—O(9)	2.656 (4)	Dy(4)—O(12)	2.374 (2)
Dy(2)—O(9^{v})	2.571 (4)	Dy(4)—O(13)	2.475 (2)
Dy(2)—O(10^{ii})	2.304 (4)	Dy(4)—O(14^{ix})	2.629 (2)
O(11^{x})—Si(1)—O(12)	106.8 (3)	O(4)—Si(3)—O(6)	114.4 (2)
O(11^{x})—Si(1)—O(13^{xi})	103.1 (2)	O(4)—Si(3)—O(7)	103.3 (2)
O(11^{x})—Si(1)—O(14^{vi})	116.8 (2)	O(5)—Si(3)—O(6)	104.8 (2)
O(12)—Si(1)—O(13^{xi})	113.6 (2)	O(5)—Si(3)—O(7)	109.0 (2)
O(12)—Si(1)—O(14^{vi})	114.9 (2)	O(6)—Si(3)—O(7)	109.7 (2)
O(13^{xi})—Si(1)—O(14^{vi})	101.1 (2)	O(7)—Si(4)—O(8)	103.2 (2)
O(1)—Si(2)—O(2)	107.6 (2)	O(7)—Si(4)—O(9^{xi})	107.6 (2)
O(1)—Si(2)—O(3)	109.4 (2)	O(7)—Si(4)—O(10)	110.2 (2)
O(1)—Si(2)—O(4)	111.0 (2)	O(8)—Si(4)—O(9^{xi})	102.7 (2)
O(2)—Si(2)—O(3)	118.8 (3)	O(8)—Si(4)—O(10)	117.2 (2)
O(2)—Si(2)—O(4)	100.6 (2)	O(9^{xi})—Si(4)—O(10)	114.8 (3)
O(3)—Si(2)—O(4)	109.1 (2)	Si(2)—O(4)—Si(3)	119.7 (3)
O(4)—Si(3)—O(5)	115.7 (2)	Si(3)—O(7)—Si(4)	131.4 (3)

† Symmetry codes: (i) $1+x, y, z$; (ii) $1-x, 1-y, 1-z$; (iii) $2-x, 1-y, -z$; (iv) $1-x, -y, 1-z$; (v) $2-x, -y, 1-z$; (vi) $x, 1+y, z$; (vii) $1-x, 1-y, -z$; (viii) $1-x, 2-y, 1-z$; (ix) $1+x, 1+y, z$; (x) $x, y, z-1$; (xi) $x-1, y, z$.

Table 5
Tetrahedral (Si—O) bond distances (Å) in type B for $Dy_2Si_2O_7$ and $Ho_2Si_2O_7$.

	$Dy_2Si_2O_7$ this study	$Ho_2Si_2O_7$ this study	$Ho_2Si_2O_7$ Felsche (1972)
Si(1)—O(11)	1.602 (4)	1.623	1.564
Si(1)—O(12)	1.610 (3)	1.598	1.560
Si(1)—O(13)	1.616 (3)	1.605	1.697
Si(1)—O(14)	1.673 (3)	1.680	1.715
Si(2)—O(1)	1.600 (4)	1.588	1.555
Si(2)—O(2)	1.652 (4)	1.673	1.595
Si(2)—O(3)	1.582 (3)	1.588	1.639
Si(2)—O(4)	1.744 (4)	1.725	1.782
Si(3)—O(4)	1.635 (4)	1.653	1.541
Si(3)—O(5)	1.630 (3)	1.641	1.592
Si(3)—O(6)	1.542 (3)	1.556	1.633
Si(3)—O(7)	1.688 (4)	1.663	1.746
Si(4)—O(7)	1.665 (4)	1.688	1.642
Si(4)—O(8)	1.665 (4)	1.665	1.568
Si(4)—O(9)	1.588 (3)	1.597	1.689
Si(4)—O(10)	1.630 (4)	1.638	1.713

The type B structure of $Dy_2Si_2O_7$ (Tables 3–5; Figs. 1 and 3–5) is seen to be very similar to that of $Ho_2Si_2O_7$ (Felsche, 1972; see Tables 1 and 5), when the correct unit-cell angles are used for the latter structure. A mixture of real space unit-cell edge lengths and reciprocal space angles were given in Felsche (1972), and were evidently used for calculating the reported bond distances. In addition, the structural parameters for $Ho_2Si_2O_7$ may have been refined using the reciprocal space angles, but the error here is likely to be minimal, because comparison refinement of the $Dy_2Si_2O_7$ structure using the reciprocal space unit-cell angles resulted in insignificant change in R values and atomic coordinates.

The silicate component of the type B structure of $Dy_2Si_2O_7$ comprises a one-to-one mixture of linear triple tetrahedral groups [Si_3O_{10}] and single (isolated) tetrahedra [SiO_4], as reported in Felsche (1972) for $Ho_2Si_2O_7$, rather than the expected diorthosilicate groups. The Si—O bond distances and O—Si—O bond angles do show some divergence from the average values for [SiO_4] tetrahedra in silicates, but the overall ranges of 1.54–1.74 Å and 100.6–118.8° are similar to those of the type B structure of $Ho_2Si_2O_7$ (*e.g.* Table 5), the topologically related silicate kilchoanite ($Ca_6Si_3O_{10}SiO_4$; Taylor, 1971) and the moderate temperature type A structure of $Pr_2Si_2O_7$ (Felsche, 1971), and reflect distortion in response to structural accommodation of large cations. Dysprosium is accommodated in irregular coordination polyhedra; one sixfold coordinated position [Dy(3); Fig. 5] and three eightfold coordinated positions. The nearest-neighbour environment of Dy(4) is particularly irregular, approaching hemispherical, and backs onto a structural channel parallel to the *b* axis (Fig. 4). Although all four Dy positions are coordinated to O atoms of both the silicate units, Dy(2) and Dy(3) principally cross-link the linear [Si_3O_{10}] groups, whereas Dy(1) and Dy(4) interconnect isolated [SiO_4] tetrahedra and terminal tetrahedra of the linear [Si_3O_{10}] groups (Figs. 4 and 5).

Discrepancies in the calculated bond-valence sums of O(2), O(3), O(7) and O(10), which are underbonded, and O(6), O(12) and O(13), which are overbonded (Table 6), are attributed to the structural accommodation of Dy^{3+}. The data in Table 6 were calculated with the bond-valence parameters of Brown (1981) and resulted in a global instability index (Rao *et al.*, 1998) of 0.14 v.u. They agree within error with bond valences calculated with the revised parameters of Brese & O'Keeffe (1991). However, the parameters of Brown & Altermatt (1985) yielded low bond-valence sums for Dy^{3+} (2.60–2.79 v.u.) and a global instability index of 0.20 v.u. This latter value does not indicate that the present structure of $Dy_2Si_2O_7$ is incorrect. Rather, the bond-valence parameters for Dy^{3+} appear to be highly dependent on the structures used in their calibration. This conclusion may be extended to other REE^{3+} cations, and is in general agreement with the discussion on REE disilicates below. We recognize that the present structure of $Dy_2Si_2O_7$ is based on measurements on a strained crystal (Fig. 2), which must contribute significantly to the high value of the global instability index (*cf.* Rao *et al.*, 1998).

As noted by Felsche (1972), linear [Si_3O_{10}] tetrahedral groups are rare in silicates (*e.g.*, Liebau, 1985) and have been reported only in the type B structure, ardennite {Mn_2^{2+}-$(Mn^{2+},Ca)_2(AlOH)_4[(Mg,Al,Fe^{3+})OH]_2(As,V)O_4Si_3O_{10}(SiO_4)_2$; Donnay & Allmann, 1968} and kilchoanite, and additionally suggested by Taylor (1971) to be present in the compound $Ca_8Si_5O_{18}$, which can be reorganized to $Ca_8Si_3O_{10}(SiO_4)_2$. Kilchoanite is a disilicate and its structure is topologically analogous to the type B structure of $Dy_2Si_2O_7$, but accommodates three large cations per disilicate formula compared

Table 6
Bond valences for $Dy_2Si_2O_7$ (after Brown, 1981).

	Dy(1)	Dy(2)	Dy(3)	Dy(4)	Si(1)	Si(2)	Si(3)	Si(4)	Σ
O(1)	0.46			0.55		1.09			2.1
O(2)	0.12	0.23		0.41		0.94			1.7
O(3)	0.44			0.25		1.14			1.83
O(4)			0.34			0.73	0.99		2.06
O(5)		0.48	0.58				1		2.06
O(6)		0.55	0.46				1.28		2.29
O(7)							0.85	0.91	1.76
O(8)		0.43	0.39	0.25				0.91	1.98
O(9)		0.17	0.43					1.12	1.94
		0.22							
O(10)	0.34	0.49						1	1.83
O(11)	0.39			0.51	1.08				1.98
O(12)			0.71	0.4	1.06				2.17
O(13)	0.45	0.36		0.3	1.04				2.15
O(14)	0.45	0.49		0.19	0.89				2.02
Σ	3.01	3.06	2.91	2.86	4.07	3.9	4.12	3.94	

with only two in the REE disilicate. This is an immediate explanation for the structural channels along *b* in the type B structure (Fig. 4). The kilchoanite structure is more efficiently packed than the type B structure, having strips of olivine-derivative γ-Ca_2SiO_4 structure alternating with strips of $Ca_4Si_3O_{10}$ composition, and Ca occupying three octahedral and one irregular eightfold coordinated positions (Taylor, 1971).

The stability of a one-to-one mixture of linear triple tetrahedral groups $[Si_3O_{10}]$ and single (isolated) tetrahedra $[SiO_4]$ requires some explanation in view of the common occurrence of the diorthosilicate group in disilicates of diverse composition. In kilchoanite, the condensed silicate group provides terminal $[SiO_4]$ tetrahedra for the stable strip of γ-Ca_2SiO_4 structure and creates a strip of structure with a lower density of Ca^{2+} cations. The chemical composition and structure of ardennite are complex (Donnay & Allmann, 1968) and an explanation for the stability of the $[Si_3O_{10}]$ group here is uncertain, although it may be related simply to polyhedral packing considerations. In the type B structure, formation of the $[Si_3O_{10}]$ group creates a variety of large cation positions and allows for a more continuous transition in the mean size of $REE^{3+}O_n$ polyhedra in the 4*f* transition metal series (*e.g.* Fig. 6). The trivalent REE are hard Lewis acids and are well known to closely approximate hard shell cations in oxide structures, and their ionic radii decrease monotonically with an increase in atomic number through the lanthanide series. The crystal chemistries of the REE disilicates crystallized at 1 bar are constrained by the spatial accommodation of REE^{3+} cations. For high-temperature REE disilicate structures the non-equivalent REE^{3+} positions labelled by coordination number are: 6 (and near octahedral) in type C (Lu, Yb and Tm); 6 in type D (Er and Ho); 7 and 7 in type E (Ho, Dy, Tb, Gd and Eu); 7, 7, 8 and 8 in type F (Eu and Sm); and 8 and 8 in type G (Sm, Nd, Pr, Ce and La); whereas, for moderate-temperature disilicate structures the coordinations are: 6 (and near octahedral) in type C (Lu, Yb, Tm, Er and Ho); 6, 8, 8 and 8 in type B (Er, Ho, Dy, Tb, Gd and Eu); and 7, 7, 9 and 9 in type A (Eu, Sm, Nd, Pr, Ce and La). We have used the left-to-right sequence of decreasing atomic number (Lu–La) to be consistent with the phase diagram of Felsche (1970*a*). Thus, the disilicate structures of the middle REE are more complex and allow for a more progressive increase in polyhedral size, with a decrease in atomic number. This tendency is naturally more exaggerated for the lower temperature phases (and structure types).

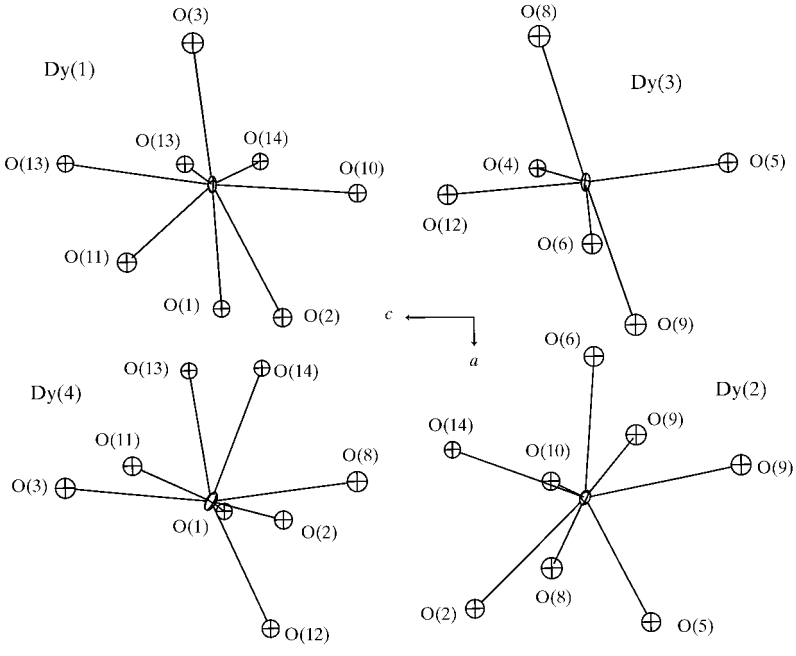

Figure 5
Coordination environment of Dy positions in $Dy_2Si_2O_7$. Thermal ellipsoids for Dy atoms are scaled to enclose 50% probability; [010] projection; drawn with *ORTEP*3 (Farrugia, 1999).

Mean bond distances ($\leq$ 2.8 Å) in the REE disilicates are compared with the effective bond distances for six-, seven-, eight- and ninefold coordination of REE^{3+} with oxygen in Fig. 6. Shannon's (1976) data for effective cation sizes were obtained by averaging mean bond distances for a very wide variety of REE compounds and structures. Not surprisingly, the present data for the limited number of REE disilicate structure types exhibit discontinuities representing the limits of accommodation by individual structure types. There is a tendency for structure types to define mean REE—O bond distances, which tend to be greater than the sum of Shannon's (1976) effective cation–anion radii at the lower end of the cation size

range of a given structure type and correspondingly smaller at the higher end. It is clear that the bond-valence requirement of the O atoms is a secondary consideration in these structures and, indeed, many O atoms in the type B structure have bond-valence sums differing significantly from 2.0. Also, the range in coordination number and details of the nearest-neighbour coordination spheres of an individual structure type are relatively unimportant as long as the mean coordination number is broadly consistent with the trend for increase in cation size and coordination number from Lu to La.

We thank Michael Jennings and the Department of Chemistry for collection of reflection intensities, Y. Thibault for assistance with EPMA, and the Natural Sciences and Engineering Research Council of Canada for financial support to MEF.

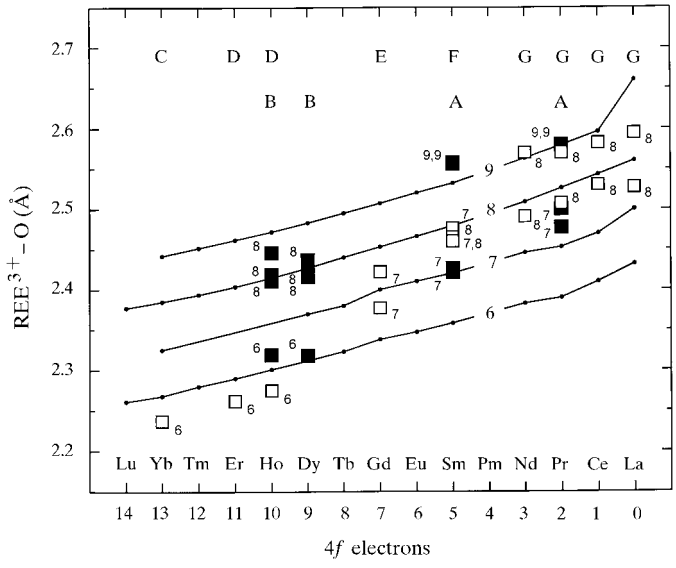

Figure 6
Mean REE—O bond distances of non-equivalent polyhedra in seven structure types (A–G) of REE disilicates, relative to the sum of the effective cation–anion radii for coordination numbers 6, 7, 8 and 9 (Shannon, 1976). Open squares are structures of high-temperature phases (top row of structure-type labels) and full squares are structures of moderate-temperature phases, including the type B structure of $Dy_2Si_2O_7$; subscripts and superscripts are coordination numbers.

References

Blessing, R. H. (1995). *Acta Cryst.* A**51**, 33–38.
Blessing, R. H. (1997). *J. Appl. Cryst.* **30**, 421–426.
Brese, N. E. & O'Keeffe, M. (1991). *Acta Cryst.* B**47**, 192–197.
Brown, I. D. (1981). *Structure and Bonding in Crystals*, edited by M. O'Keeffe and A. Navrotsky, Vol. II, pp. 1–30. New York: Academic Press.
Brown, I. D. & Altermatt, D. (1985). *Acta Cryst.* B**41**, 244–247.
Christensen, A. N. (1994). *Z. Kristallogr.* **209**, 7–13.
Christensen, A. N. & Hazell, R. G. (1994). *Acta Chem. Scand.* **48**, 1012–1014.
Christensen, A. N., Hazell, R. G. & Hewat, A. W. (1997). *Acta Chem. Scand.* **51**, 37–43.
Christensen, A. N., Jensen, A. F., Themsen, B. K., Hazell, R. G., Hanfland, M. & Dooryhee, E. (1997). *Acta Chem. Scand.* **51**, 1178–1185.
Coppens, P. (1977*a*). *DATAP*77. State University of New York, Buffalo, USA.
Coppens, P. (1977*b*). *LINEX*77. State University of New York, Buffalo, USA.
Coppens, P., Leiserowitz, L. & Rabinovich, D. (1965). *Acta Cryst.* **18**, 1035–1038.
Dias, H. W., Glasser, F. P., Gunwardane, R. P. & Howie, R. A. (1990). *Z. Kristallogr.* **191**, 117–123.
Donnay, G. & Allmann, R. (1968). *Acta Cryst.* B**24**, 845–855.
Dowty, E. (1995). *ATOMS for Windows.* Version 3.1. Shape Software, 521 Hidden Valley Road, Kingsport, TN 37663, USA.
Farrugia, L. J. (1999). *ORTEP*3 *for Windows*. University of Glasgow, Scotland.
Felsche, J. (1970*a*). *J. Less-Common Met.* **21**, 1–14.
Felsche, J. (1970*b*). *Naturwiss.* **57**, 452.
Felsche, J. (1970*c*). *Naturwiss.* **57**, 669–670.
Felsche, J. (1971). *Z. Kristallogr.* **133**, 364–385.
Felsche, J. (1972). *Naturwiss.* **59**, 35–36.
Fleet, M. E. & Burns, P. C. (1990). *Can. Mineral.* **28**, 719–723.
Fleet, M. E., Liu, X. & Pan, Y. (2000). *Am. Mineral.* In the press.
Greis, O., Bossemeyer, H. G., Greil, P., Breidenstein, B. & Haase, A. (1991). *Mater. Sci. For.* **79–82**, 803–808.
Liebau, F. (1985). *Structural Chemistry of Silicates.* Berlin: Springer-Verlag.
Nonius (1997). *Collect Software.* Nonius, Delft, The Netherlands.
Rao, G. H., Bärner, K. & Brown, I. D. (1998). *J. Phys. Condens. Matter*, **10**, L757–L763.
Sewell, D. A., Love, G. & Scott, V. D. (1985) *J. Phys. D*, **18**, 1233–1243.
Shannon, R. D. (1976). *Acta Cryst.* A**32**, 751–767.
Siemens (1993). *SHELXTL/PC.* Version 4.1. Siemens Analytical X-ray Instruments, Inc., Madison, WI 53719, USA.
Smolin, Yu. I. & Shepelev, Yu. F. (1970). *Acta Cryst.* B**26**, 484–492.
Smolin, Yu. I., Shepelev, Yu. F. & Butikova, I. K. (1970). *Sov. Phys. Cryst.* **15**, 214–219.
Taylor, H. F. W. (1971). *Mineral. Mag.* **38**, 26–31.
Tunell, G. (1952). *Am. J. Sci.* Bowen volume, 547–551.